Street Tracking Based on SAR Data from Urban Areas

Sigurjon Orn Sigurjonsson
Jon Atli Benediktsson
and Johannes R. Sveinsson
Department of Electrical and
Computer Engineering
University of Iceland
Hjardarhaga 2-6, 107 Reykjavik, Iceland
sigurjs@ieee.org, {benedikt, sveinsso}@hi.is

Gianni Lisini
and Paolo Gamba
Department of Electronics
University of Pavia
Via Ferrata 1, 27100, Pavia, Italy
{gianni.lisini, paolo.gamba}@unipv.it

Jocelyn Chanussot
Signal & Images Laboratory - LIS/INGP
BP 46 - 38402
St. Martin d'Heres, France
jocelyn.chanussot@lis.inpg.fr

***Abstract*— A method for street tracking is proposed. The method consists of two steps. First, a "blob image" of possible street candidates is created. Then, the street segments from that blob image are extracted. Two feature extraction approaches based on mathematical morphology are applied as preprocessing for the street tracking. One method is based on using differential morphological profiles but the other uses morphological opening and closing operators with a rotating structuring element (SE). The method is tested on an AIRSAR image from Los Angeles with and without noise filtering. The obtained results are measured using two indexes; correctness and completeness. Of the two methods used in the feature extraction, the SE rotation appears to give better results. Noise filtering does not have a major effect in street tracking for the AIRSAR image.**

I. Introduction

Classification of high-resolution remote sensing images from urban areas has been addressed in [1] and [2] using two main steps:
- feature extraction based on the construction of a differential morphological profile (DMP) which characterizes each pixel both in terms of intensity and in terms of local geometry and
- classification based on a neural network (eventually after selection of the most significant features).

In this paper, a further evolution of [1] and [2] is presented and applied in neural network classification of an AIRSAR image of Los Angeles, California shown in Fig. 1. For the feature extraction step, two methods are used. One applies openings and closings with linear structuring elements under varying angles and the other creates Differential Morphological Profiles as described in [1]. The effect of using speckle filtering prior to the construction of the morphological profiles is also investigated, as is the effect of Alternating Sequential Filters, a family of morphological filters.

The maps obtained from the classification of the different morphological profiles are used for street tracking. The street extraction is done in two steps. The first one is aimed at discarding the blobs that do not possess the usual characteristics of the roads such as elongation. This is made by a routine that tries and associate each blob present in the filtered image to a "street prototype" database [3]. If the shape of the blob under test is too different from the ones found in the database, it will be removed from the image. It is possible to remove even only a part of the entire blob that shows too peculiar features. The second step is a skeletonization step reducing the selected blobs to linear segments.

To evaluate the quality of the extracted street network, two quantitative indexes are computed, the correctness and completeness indexes [4]. Both of them require the knowledge of the true network and provide a means to understand to what extent the extracted network is similar to the reference one. In particular, completeness represents the fraction of ground truth length extracted while correctness is the fraction of segments' length belonging to actual roads.

II. Feature Extraction

This section describes two different methods used for feature extraction which - although they are referred to as such - they are actually classification methods themselves. They both rely on neural networks and differ only in the way the input vectors are constructed. On one hand they are created using *Differential Morphological Profiles* [1] (DMPs) and on the other using morphological openings and closings with linear structuring elements under various angles.

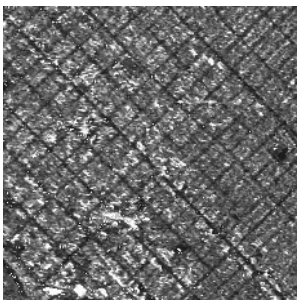

Fig. 1. AIRSAR image of Los Angeles, California.

0-7803-9050-4/05/$20.00 ©2005 IEEE.

A. Openings and Closings Under Various Angles

Let

$$\theta_k = k\frac{\pi}{15} \qquad k = 0, \ldots, 14 \tag{1}$$

define 15 equally spaced angles between 0 and π and S_{θ_k} be a linear structuring element (SE) of an arbitrary, but static, length that forms an angle θ_k with the vertical axis. Define $\Gamma^I_{\theta_k}(\mathbf{x})$ and $\Phi^I_{\theta_k}(\mathbf{x})$ as the morphological openings and closings [5], respectively, of the image I using the SEs S_{θ_k} at pixel $\mathbf{x}$. The feature vector used for the neural network classification is made up of the terms

1. $BTH(I)$
2. $\max_k \left[\Gamma^I_{\theta_k}(\mathbf{x})\right]$
3. $\max_k \left[\Phi^I_{\theta_k}(\mathbf{x})\right]$
4. $\max_k \left[\Gamma^I_{\theta_k}(\mathbf{x})\right] - \min_k \left[\Gamma^I_{\theta_k}(\mathbf{x})\right]$
5. $\max_k \left[\Phi^I_{\theta_k}(\mathbf{x})\right] - \min_k \left[\Phi^I_{\theta_k}(\mathbf{x})\right]$

where $BTH(I)$ is the *black top-hat* of I which is defined as the arithmetic difference between the closing of I and the image itself [5], $BTH(I) = \phi(I) - I$. The SE rotation for

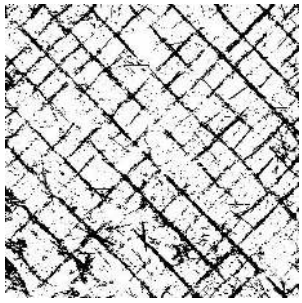

Fig. 2. Neural network classification results of the unfiltered image.

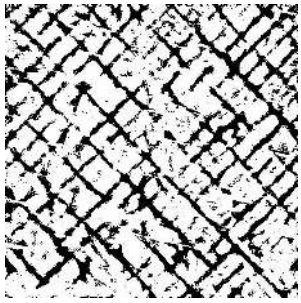

Fig. 3. Neural network classification results of the Frost filtered image.

$k = 1, \ldots, 15$ is shown in Fig. 4. There we see the openings of the AIRSAR image with a linear SE of the length of 30 pixels under 15 different angles. When the SE is more or less aligned to a street, that particular image structure is highlighted and others inhibited. Figs. 2 and 3 show the results of the neural network classification when applied to the SAR image unfiltered and after being filtered with a Frost filter [6] to reduce speckle noise. The image was also prefiltered using an Alternating Sequential Filter (ASF) [5]. If γ_i is an opening of

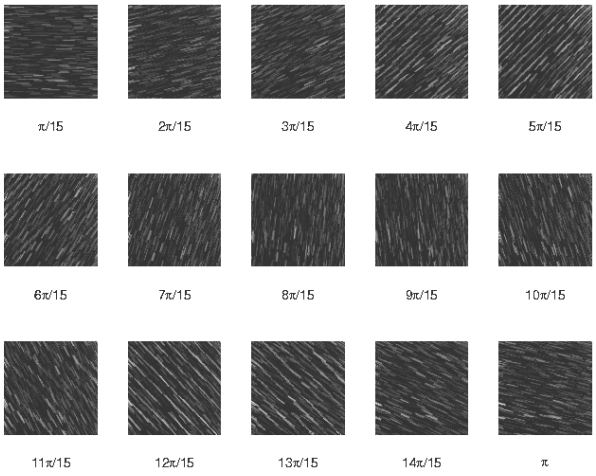

Fig. 4. Openings of the AIRSAR image with a linear SE under varying angles.

size i and ϕ_i is the dual closing, then

$$M_i = \gamma_i\phi_i \ldots \gamma_2\phi_2\gamma_1\phi_1 \tag{2}$$

and

$$N_i = \phi_i\gamma_i \ldots \phi_2\gamma_2\phi_1\gamma_1 \tag{3}$$

are both ASFs of size i [5]. The black regions of the images in Figs. 2 and 3 are pixels that have been classified as streets. These are merely tentative classifications, though. A street extraction algorithm is applied to the binary images obtained here, and is described in Section III.

B. DMPs

Applying openings and closings on an image I using circular SEs with increasing size, we can form the vector

$$\Pi(I) = [\phi_n(I), \ldots, \phi_1(I), I, \gamma_1(I), \gamma_n(I)]\,. \tag{4}$$

The DMP is simply the difference vector of $\Pi(I)$ [1]. It is not essential to use the difference vector but, of course, it is one dimension smaller than $\Pi(I)$. The way pixels react to the openings and closings reflects the spatial characteristics of the image structures to which they belong. DMPs are described in detail in [1].

III. Street Extraction

This step aims at simplifying the previously classified image where street candidates are depicted as black blobs of different shapes in a white surrounding. After discarding uninteresting blobs, the method is able to check if the remaining ones have all the characteristics of streets or part of them. The overall procedure is divided into three separate steps. The first one detects the parts of the image where the road candidates may be present. The algorithm divides the image into several sub-windows containing both pixels classified as belonging to a road and/or to the background. The initial window size is arbitrary. The second step tests every sub-area counting the number of black pixels in them.

If the ratio of black to white pixels is higher than a specified threshold the windows will be enlarged with the intent of reducing this percentage. If this is not possible, the sub-area is discarded. The position of the sub-windows can also be altered in order to get the best symmetrical position of the blob. The third step aims at discarding part of the image under test assuming that a street is a curvilinear border between two blobs with indefinite shapes and in order to do this we have to determine the number of blobs in the sub-window. This is done by performing a double diagonal scan of the sub-area counting the number of black to white pixel changes (road to background or vice-versa). If the test is passed additional checks are performed to even further reduce the number of street candidates. These check the filling ratio, edge parallelism and finally adjust the window in both width and position within the image to "optimally" check the inside blob. The last step is represented by a tracking procedure with the aim of connecting parts of the same blob. After identifying all possible blobs, each of them is compared to a set of 16 basic prototypes (which cover all possible road directions). This discards blobs that do not show a close similarity with the aforementioned prototypes by looking at their edges and commuting the number of pixels in the blob "outside" the prototype. This number is inversely related to the probability that the tested blob represents a linear element in the image (which we assume is a part of a road). The final blobs maintain a record of information:

- **Quality**: the error function value;
- **Direction**: the mean direction of the pixels belonging to the identified road;
- **Thickness**: the difference of the two minimum positions;
- **Length**: determined by the dimension of the image square portion.

IV. Experimental Results

The proposed procedure was applied to an AIRSAR image of Los Angeles, California applying the line detector on the pre-computed images like the ones described in Section II. The original image was taken on August 5, 1994, from the height of 11,000 m, and has a spatial resolution of 5 meters/pixel. Examples of couples of pre-computed images and extracted images are shown in Figs. 5 and 6. The left columns show the results of the feature extraction algorithm of Section II and the right show the results of the street extraction algorithm of Section III. For the assessment of the street extraction we use two different indexes: a) the completeness that represents the fraction of the length of the extracted data and b) the correctness is the fraction of segment length belonging to actual roads. Table I shows these indexes for several images while the reference data are depicted in Fig. 7. The expressions $8-2$ and $8-4$ in Table I indicate how the DMP was created. Here, 8 is the number of openings and closings applied and 2 and 4 are the SE size increments. "ASF_7 (γ)" means that the size of the ASF was 7 and that it begins with an opening, i.e. the filter in (3) was used. Likewise, "ASF_7 (ϕ)" means that the filter in (2) was used.

TABLE I

Correctness and completeness indexes. The tables show the results for the SE rotation method (upper) and the DMP method (lower).

SE rotation				
Image	ASF_7 (ϕ)	ASF_7 (γ)	Frost	Unf.
Corr.	0.61	0.60	0.67	0.68
Compl.	0.66	0.68	0.73	0.72

DMP			
Image	Frost 8-4	Unf. 8-2	Unf. 8-4
Corr.	0.68	0.72	0.62
Compl.	0.66	0.59	0.80

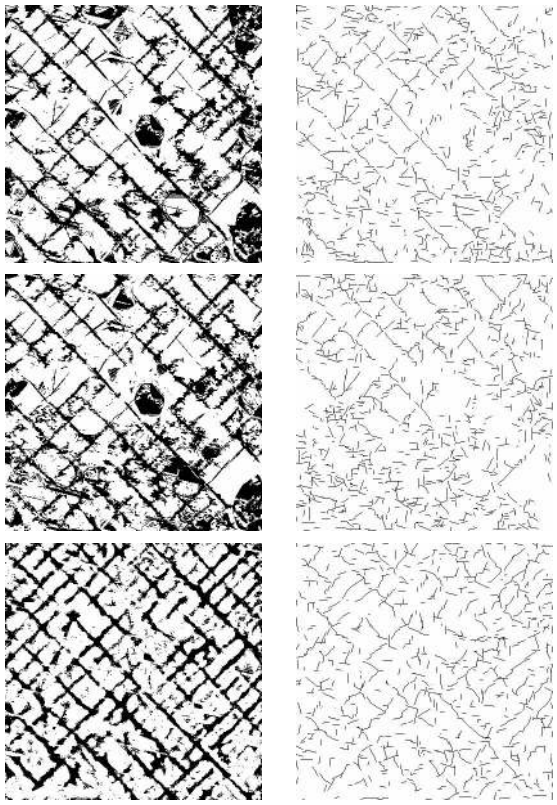

Fig. 5. Results of feature extraction (left) and street tracking (right) using ASF (top and middle) and Frost filters (bottom). SE rotation was used in all these cases.

The correctness and completeness are both ratios so they will take values between 0 and 1 where higher values translate to more accurate results. In Table I, it is interesting to note that the noise filtering does not have a substantial effect on the index values. In fact, in the case of the SE rotation method the results are worse when ASFs are used - relative to the unfiltered case. But visually - looking at Fig. 5 - the most satisfying result seems to be the case where the Frost speckle filter was applied to the image prior to classification. After

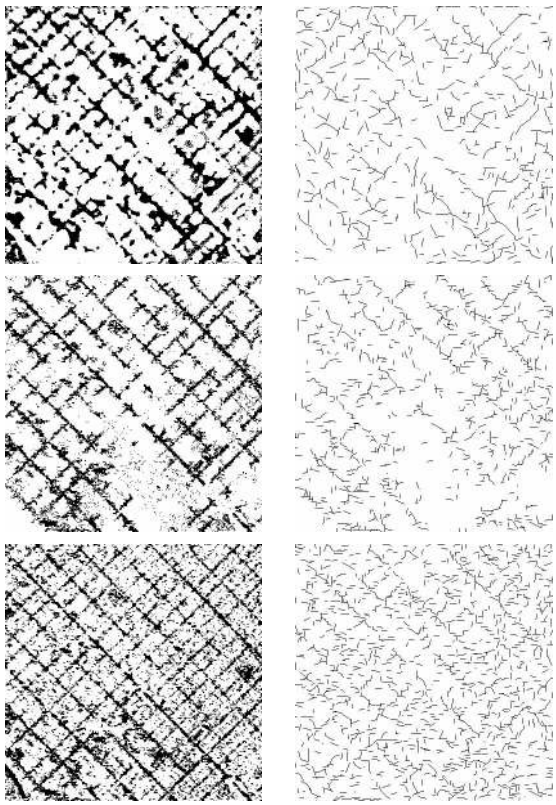

Fig. 6. Outcome of feature extraction (left) and street tracking (right), Frost filtered (top) and unfiltered (middle and bottom). DMPs were used in all these cases. The DMP parameters are $8-4$ (top and bottom) and $8-2$ (middle).

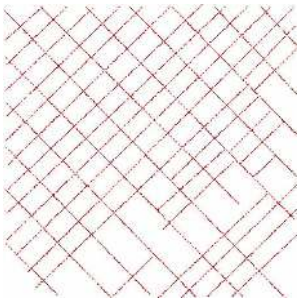

Fig. 7. The reference data.

all, the Frost filter is designed to preserve edges [6]. As a result, the output of the feature extraction stage contains fewer irrelevant, non street-shaped blobs, as can be seen in Fig. 5. The SE rotation combined with the Frost filter also does a better job than the DMP method, judging from Fig. 6. The blob image from the SE rotation method is cleaner and more structured, as are the extracted street segments. It is rather difficult to percieve any structure at all from the image in the bottom row of Fig. 6. Of course, the strength of the SE rotation lies in the fact that using a linear SE, we can highlight long and narrow image structures, which streets certainly are, while the DMP method uses circular SEs [1].

V. Conclusion

A method of extracting the street network from a high-resolution AIRSAR image of urban areas was proposed. The method consists of two steps, a feature extraction step relying on mathematical morphology and a street tracking step that analyzes the binary image constructed by the feature extraction. Of the two methods used in the feature extraction step, the SE rotation appears to give better results which are in turn made even better by pre-applying the Frost filter to the original image. Future exploration and development of the method might include permitting the SE element length to vary in some way. While the image used in this paper contains only straight street segments, that is generally not the case. An implementation of the SE rotation with variable SE lengths might be better equipped to deal with sharp turns.

Acknowledgment

The authors would like to thank Dr. B. Houshmand for providing the AIRSAR data of Los Angeles, CA. The work was partially supported by the Icelandic Research Council and the Research Fund of the University of Iceland.

References

[1] M. Pesaresi and J. A. Benediktsson, "A new approach for the morphological segmentation of high-resolution satellite imagery," *IEEE Transactions on Geoscience and Remote Sensing*, vol. 39, no. 2, pp. 309–320, Feb. 2001.

[2] J.A. Benediktsson J.A. Palmason and J.R. Sveinsson, "Classification of hyperspectral data from urban areas based on extended morphological profiles," *IEEE Transactions on Geoscience and Remote Sensing*, vol. 43, no. 3, pp. 480–491, 2005.

[3] F. Dell Acqua P. Gamba and G. Lisini, "Road map extraction by multiple detectors in fine spatial resolution SAR data," *Canadian J. Remote Sensing*, vol. 29, no. 4, pp. 481–490, Aug. 2003.

[4] C. Wiedermann and H. Ebner, "Automatic Completion and Evaluation of Road Networks," *Int. Arch. Photogramm. Remote Sensing*, vol. 33, pp. 976–986, 2000.

[5] P. Soille, *Morphological Image Analysis - Principles and Applications*, Springer Verlag, Berlin, Germany, 2nd edition, 2003.

[6] Y. Yu and S. T. Acton, "Speckle reducing anisotropic diffusion," *IEEE Transactions on Image Processing*, vol. 11, no. 11, pp. 1260–1270, Nov. 2002.